Analysis of scour depth in the case of parallel bridges using HEC-RAS

Darshan J. Mehta and S. M. Yadav

ABSTRACT

Scour is now one of the main problems for river as well as for coastline engineering. Bridges are the vital structures which must be designed to prevent failure against the effects of scour. Scour holes can occur without warning and cause the failure of a bridge. The main significant issues in hydraulic and river engineering are to determine the connection between parameters affecting the maximum and minimum depth of scour. The scour depth in the alluvial stream below a river bed differs based on the flows, pier shape, pier size and sediment characteristics. Dual bridges of basically the same structure are placed parallel to and only a small distance away from an existing bridge, either on the upstream or downstream side. Naturally, the backwater generated by dual bridges is bigger than that of a single bridge but lower than the value resulting from separate consideration of the two bridges. In the present work, an hydraulic model is used to simulate the stability of a bridge in the study area, namely 'Sardar Bridge' on the Tapi river. Scour profiles for various flood events have been assessed for a particular bridge. The velocity of flow is used to estimate depths of scour at different piers and abutments. Estimating depth of the scour during the design can significantly decrease the overall cost of bridge foundation construction. Results from the present study show that construction of a new bridge should be proposed on the upstream side rather than downside side of the existing bridge. By doing so, hydraulic stability of the existing bridge is ensured.

Key words | bridge, flood events, HEC-RAS, scour depth

Darshan J. Mehta (corresponding author)
S. M. Yadav
Civil Engineering Department,
SVNIT,
Surat, Gujarat,
India
E-mail: *darshanmehta2490@gmail.com*

HIGHLIGHTS

- Effect of parallel bridge on an existing bridge.
- Numerical simulations carried out around and on bridge piers for the local scour.
- Explored variation in depth of scour and its effect for adjacent bridges.
- Estimating the scour during bridge design, reduces the overall cost of bridge foundation constructon.
- Hydraulic modeling is carried to simulate and check stability of bridge in the study area.

INTRODUCTION

The term bridge scour describes the loss of bed materials as a result of the turbulent impact of water flowing around the supports of a bridge. Bridge pier foundations can be destabilized if excessive scouring occurs, potentially resulting in bridge failure. Bridge scour evaluation techniques used for erosion-resistant materials are qualitative and unreliable or quantitatively over conservative (Ansari & Qadar 1994) Bridges have always been a big challenge for engineers and builders, both in their design stage and in maintaining their stability. Scour is defined as the reduction of the river bed by water erosion that may lead to the exposure of the bridge foundation

doi: 10.2166/ws.2020.255

(Azamathulla *et al.* 2013). Bridge failure history reveals that the majority of events took place because of design that failed to properly account for the ability to erode alluvial river bed material, or to scour the channel bed and banks. Images of damaged/broken piers, undercut piers and failed bridge methods have long troubled bridge designers and structural engineers (Afzali 2016). Furthermore, the engineers who built them were considered a type of high priest (the word Pontifex comes from the Latin Pontem Facere that means 'to build bridges'), acting as mediators between Gods and believers (Baker 1980). Flow pattern modifications trigger an increase in sediment motion that leads to the scour phenomenon. Understanding the phenomenon of bridge pier scouring is of paramount interest to the hydraulic engineering industry as bridge failure can happen without a thorough understanding, leading in loss of lives and catastrophic devestation (Pandey *et al.* 2020, 2020b). Scour depth is a key parameter to determine the minimum foundation depth as it decreases the foundation's capacity. This is why comprehensive experimental research has been carried out in an effort to comprehend the complicated process of scouring and to determine a technique of predicting depth of scouring for different pier circumstances (Beg & Beg 2013). Precisely predicting scour depths for new bridges under flood events is essential: underestimating scour depths can lead to expensive bridge repairs or even disastrous bridge failures, while overestimating can lead to expensive, unnecessarily deep foundations (Pandey *et al.* 2018a, 2018b). It is also essential to evaluate scour potential for existing bridges. Indeed, some of those screened critical bridges may result from scour-overestimation, due to misuse of assumptions or engineering decisions and the inaccuracy of equations for scour prediction. The main vortex system is formed by forward flow which, on collision, deviates downward (Link *et al.* 2020).

Evaluation of scour on a bridge pier was computed using the hydraulic model HEC-RAS (5.0.3). Results of this model show that in discharges with a larger return period, increases in scour, especially for bridge lateral piers, due to the discharge increase, velocity and vortex flow around the piers (Nou *et al.* 2020). Although in some cases the HEC-RAS model estimates scour more than an *in vitro* model, in general overall outcomes the models are in good agreement, so that HEC-RAS can be used in the study of bridges and their designs to assess precise scouring and depth of bridge pier (Cunha 1975; Dahe & Kharode 2015). Sometimes a long-standing channel may suddenly start moving due to some critical effects such as floods, bank material, bank vegetation and land use. Scour at the site of a bridge is normally classified as contraction and local scour (Singh *et al.* 2020). Contraction scouring happens throughout a whole area of cross-section, for instance, due to the enhanced speeds and shear stresses resulting from a contraction of the channel through a bridge growth (Yusoff *et al.* 2016). As a rule, the smaller the opening ratio, the greater is the velocity of the conduit and the greater the scouring. If flow is contracted from a broad floodplain, there may be comprehensive scouring and failure in a bank. Relatively serious constraints can involve decades of periodic maintenance to fight erosion (Debnath *et al.* 2014). It is observed that the best way to decrease contraction scour is to widen the bridge or construct a new one adjacent to the existing bridge. Scour effect takes place due to velocity and associated vortices as water strikes around the edges of projections, piers and banks of a spur (Goel 2015). The flow layout around a pier is shaped like a barrel. As it approaches, the approaching stream decelerates, stopping at the center of the pier (Gaudio *et al.* 2010; Feng *et al.* 2011). The subsequent stress is most astonishing near the water surface where the approach velocity is most prominent and it reduces gradually. The piers face a downward pressure gradient which directs the stream downwards. Local scouring occurs near the stagnation point as downstream velocity is adequately capable of overcoming the resistance of the bed particles motion (Govindasamy *et al.* 2010). During flooding, the filling behind abutments may scour, despite the reality that the bridge's foundations may not suffer loss. Usually this type of failure occurs with single bridge abutments having vertical walls (Ghanbari & Kashefipour 2017). The present research addresses the numerical simulations around and on bridge piers for local scour. This study aims to explore variation in depth of scour and its effect for adjacent bridges. The distance between two parallel bridges was increased gradually and its effect on scour depth around bridge pier was observed with the increase in the flow.

CASE STUDY: MUMBAI GOA HIGHWAY BRIDGE COLLAPSE, MAHAD MAHARASHTRA

There were two parallel bridges; one was new bridge and one constructed more than seven decades ago. The old one collapsed. Record rain in the hilly terrain of Mahabaleshwar and the catchment areas turned the usually narrow Savitri River into a torrent that washed away the British-built bridge in Mahad. The Savitri River that flows through Mahad originates in Mahabaleshwar which recorded the second highest rainfall, recording 410 mm rain in the 24 hours till 8:30am. Most of the catchment area of the Savitri and Kal rivers, which meet just ahead of the bridge in Mahad, is on the slopes of Mahabaleshwar, Shivtharghal and Dasgaon areas. Figure 1 shows the collapsed bridge, at Mahad. This specific area has a history of receiving 1,000 mm rain in 24 hours, and the intensity of the showers in the hilly areas such as Mahabaleshwar, Shivtharghal and Kal river catchment were enough to increase the river water levels by half a metre in a short time period. The Mahad taluka received 222 mm rain in the same period. The heavy showers in Mahableshwar, besides the rain in the catchment regions of the river along the Mahabaleshwar to Mahad route, flooded the river. Figure 2 shows the location of the bridge on the meandering river and the newly constructed bridge on the upstream side of the old bridge. The primary reason for failure of the bridge seems to be the high pressure caused by flood in the river Savitri and heavy rains in the catchment of Mahabaleshwar.

Figure 1 | Collapsed Bridge, Mahad. *Source*: timesofindia/bridge-collapse-on-goa/liveblog.

STUDY AREA AND DATA COLLECTION

Study area

On the Indian Peninsula, Tapi River is the second biggest river flowing west. It originates in the district of Multai in Betul, 752 meters above sea level in Madhya Pradesh, and is 724 km long. It has large tributaries on both banks, with the 14 main tributaries being over 50 km long. Four of them are on the right bank: Vaki, Gomai, Arunavati and Aner. Ten major tributaries are on the left bank and drain into the primary river channel, namely the Nesu, Amaravati, Buray, Panjhra, Bori, Girna, Waghur, Purna, Mona and Sipna. The shape of the basin is elongated with a maximum length of 687 km from east to west and a maximum width of 210 km from north to south. Surat city is situated in the delta region of the Tapi river and has a history of frequent

Figure 2 | (a) Location of the bridge on the meandering river, (b) New bridge constructed later on the upstream side of the old bridge.

flooding. The Tapi basin is split into three sub basins, namely the upper Tapi basin (up to Hathnur), the middle Tapi basin (from Hathnur to Gighade) and the lower Tapi basin (from Gighade to the sea). The Sardar Bridge is situated in the center of Surat city. It is 50 m long. It has nine piers. Figures 3(a) and 3(b) show the pier of the existing Sardar Bridge in Surat city. Since it is in the center of the city, the Surat municipal corporation decided to add two lanes on either side of the existing bridge (which already has four lanes). The following are the study reach details: number of cross-sections are 10 (CS-1 to CS-10), study reach length is 3 km (3,000 m), average distance from river reach cross-section to cross-section is 200 to 250 meters; see Figures 4(a) and 4(b).

Data collection

Cross-sections along the length of Tapi river and Sardar bridges were used to estimate scouring depth on and around the piers. A picture of the study area was acquired and used to operate the hydraulic model. Bed material data were collected to understand the local scour and maximum scour around bridge piers. Past peak flood data from the years 1944, 1968 and 2006, and carrying capacity of Tapi River were used to compute the depth of scour. The length of the Sardar Bridge reach modelled is 3 km. The study reach has a total 10 cross-sections. Data was collected for the present study from the locations shown in Table 1.

METHODOLOGY

The total scour consists of three parts: long-term aggradation and degradation, contraction scour, and local scour at piers and abutments. Contraction scour occurs when a natural contraction or bridge contraction of the flow decreases the flow region of the stream. Bridge opening, highway embankments, bridge abutments and bridge piers are the factors that influence contraction scour (Johnson *et al.* 2015). Pier scour is known as horseshoe vortex due to the acceleration of the

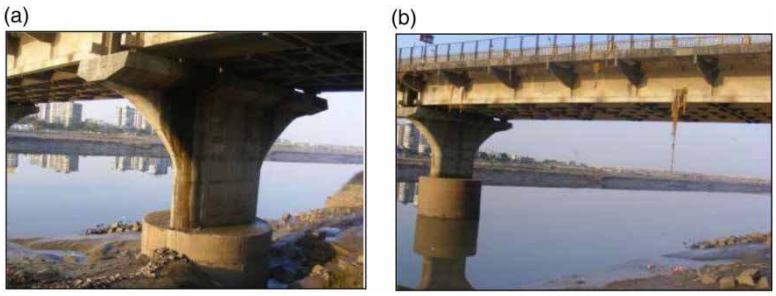

Figure 3 | (a) Study area showing bridge piers, (b) Sardar Bridge showing piers.

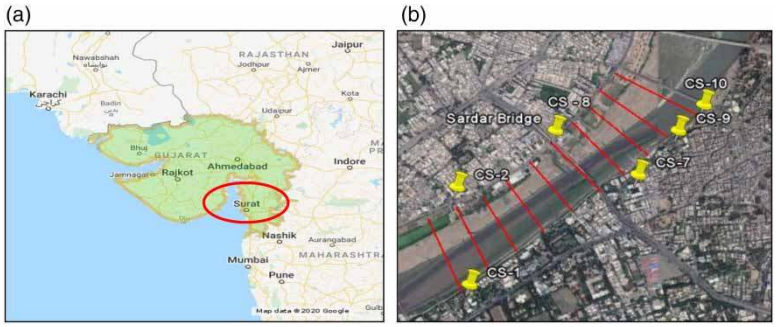

Figure 4 | (a) Map of India & Gujarat, (b) Study area with river reach cross-sections (cross-sections shown in red). Please refer to the online version of this paper to see this figure in colour: http://dx.doi.org/10.2166/ws.2020.255.

Table 1 | Data and office/location

Serial No.	Description of data collected	Office/location
1	Topographic data i.e. channel cross-sections, longitudinal cross-sections and layout	Surat Irrigation Circle, Surat
2	Bridge cross-sections i.e. pier and abutment details	Surat Municipal Corporation, Surat
3	Hydrologic data i.e. past flood data, inflow hydrograph, upstream and downstream boundary conditions and historical change data.	Surat flood cell, Surat
4	Bed material	From bank of Tapi river near Sardar Bridge

flow around the pier and the formation of stream vortices (Kandasamy & Melville 1998). The variables affecting a pier's depth of local scour are: flow velocity just upstream of the pier, flow depth, pier width, bed material gradation, shape of pier, pier length, bed configuration and approach flow angle. The equation developed by Colorado State University (CSU) in 1990, adopted by the U.S. Hydrologic Engineering Center for the assessment of bridge pier scour, duly accounts for multi fluvial impacts related to shape of pier nose, flow angle, bed configuration and particle size gradation of bed material, scour retarding bed armoring, flow depth and flow inertia of the flow represented by a Froude number along with an additional safety factor of 2 (Kester & Davis 2010). A bridge hydraulic analysis needs an evaluation of the vulnerability of the proposed bridge to scouring any existing bridge. Due to the extraordinary risk and financial hardships presented by a disastrous bridge breakdown, exceptional considerations must be given to the scour and foundation investigation of an existing bridge before the construction of any new bridge (Liu *et al.* 2009). Since the field of scour prediction and investigation is new, hydraulic engineers should always be aware of and use the latest scour research and advice available (CDOT 2019; Kumar & Kothyari 2004).

HEC-RAS was designed originally in 1995 by the United States Army Corps of Engineers Hydrologic Engineering Center's River Analysis System and is 'software that allows you to perform one-dimensional steady and unsteady flow river hydraulics calculations, sediment transport-mobile bed modelling, and water temperature analysis' (MacBroom 2012; Mousavi & Daneshfaraz 2013) This software uses Preissmann's finite difference second order scheme with an implicit linearized system to settle the mass and momentum conservation equations. The left-right overbank and channel are expected to have a similar level of water surface in a cross-section. This software has the capacity to calculate profiles of water surface for constant discharge, daily discharge with subcritical, super critical, and mixed type flow (Neerukatti *et al.* 2013). The propagation of scour to the pier's downstream depends heavily on whether the pier is aligned with the direction of flow or not. Scouring in a gravel is significantly distinct from sand sizes (Kester & Davis 2010; Hamidifar & Omid 2017). The bridge pier scour module of HEC-RAS is a mathematical model to work out the bridge scour using Equation (1).

$$D = K_1 K_2 K_3 K_4 a^{0.65} y^{0.35} F^{0.43} \quad (1)$$

where,

D = Depth of scour in meters
K_1 = Pier nose shape correction factor
K_2 = angle attack of flow correction factor
K_3 = Bed condition correction factor
K_4 = Armoring of bed material correction factor
a = Width of piers (meters)
y = Depth of flow (meters)
F = Froude number

An object's capacity to pass through water depends on its size (length and area) just like the relative velocity and depth of water. The Froude number is defined as the ratio of inertia force to gravitational force (Tyagi 2001; Yanmaz & Bulut 2001; Rodriguez *et al.* 2003; Yanmaz & Kose 2007). The higher the Froude number, the more notable the resistance applied to the stream bed material by the water stream. Relating pier scour to flow depth, discharge flow, size of pier and Froude number is a simple engineering practice (Devi & Barbhuiya 2017). It has been observed that pier scour depends on both flow depth and velocity, and because of this pier scour increases with increasing Froude number (Yu & Yu 2008; Yu *et al.* 2011). Scour depth also depends on water flow depth and velocity. In this present study, the relationship between scour depth and Froude

number is also discussed. The average velocity is assessed by considering the flow and dividing it by the flow area for each of the slices (Brandimarte *et al.* 2012). The flow rate and the gate area at the gate/inline structure can be extracted using the 'Cross-Section Output' button in the HEC-RAS main window from which the velocity can be calculated.

Scour modelling in HEC-RAS

In the present study, initially the water level profile and scour depth were modeled using required hydraulic and hydrological data using HEC-RAS. Cross-sectional data were extracted using topographic maps in AutoCAD. After preparing topographical maps, cross-sections of the river upstream and downstream were created and cross-sectional data, including main water channel and numerical cross-sectional data, were extracted and modelled using HEC-RAS. HEC-RAS input data include cross-sectional data, bed slope, Manning's coefficient, discharge with different return periods, expansion and contraction coefficient and geometric characteristics of the bridge. The system is a graphical user interface (GUI) and uses hydraulic parameters. The model is verified along with the observed water level at a particular cross-section and also calibration of the model carried out by changing the value of Manning's (n) as well as slope geometry, if the cross-sectional data of that particular area are not surveyed.

Geometric data

Cross-sectional data represent the geometry of the study reach. Cross-sections are taken at quite small span along the river to characterize carrying capacity of the river and its adjacent floodplain. Geometry of the channel, normal depth with bed slope and flow resistance are required for simulating uniform flow using a hydraulic model. In this geometric data editor window these data were incorporated. Using the bridge geometrical data menu, bridge location on the river reach was selected along with all the details of the model, as shown in Figure 5.

Bridge geometry

All the fundamental information identified with the extension is incorporated into the editor window. The position

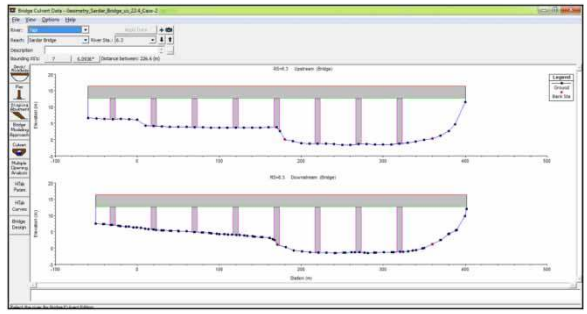

Figure 5 | Input of bridge data.

of the bridge is shown by adding a new elevation station for the bridge. The interval between the cross-section and bridge is incorporated along with details of roadway, bridge width in direction of flow, and the bridge thickness is portrayed by adding the elevation stations and details of the bridge as well as piers. The detail of piers shows the distance from the centerline of each pier and width as well as height of each pier represented by its elevation. All data related to piers and the bridge are added as input in HEC-RAS software as shown in Figure 5.

Steady flow data

To analyze steady flow, discharge of any flood event is required in order to calculate a water level profile. Steady flow data contains flow regime, normal depth, bed slope and peak discharge of that year. Flow regime classified into subcritical, supercritical or mixed flow regime is considered to carry out steady flow analysis.

The following steps should be followed to estimate bridge scour depth around the bridge pier:

Step 1: For study reach, 10 cross-sections' details such as station, elevation and Manning's (n) roughness co-efficient should be entered in the geometric data window and the files saved.

Step 2: Now go to Run window and click on 'Hydraulic design function' and then select 'Bridge scour'.

Step 3: In the Bridge scour window enter the value of d_{50} bed material size which is needed to calculate contraction scour.

Step 4: In the same window, go to pier details and select the shape of Pier. In the present study, bridge piers were V shaped.

Step 5: Add proposed bridge adjacent to existing bridge at a distance of 11.2 m, 56 m, 100.8 m and 145.6 m upstream and downstream.

Step 6: Enter steady flow data i.e. peak discharge and reach boundary conditions. In the present study 33257 cumecs (m^3 s^{-1}) (1944), 25788 cumecs (2006), 43924 cumecs (1968) were used for flood events and 8501 cumecs was used as as the carrying capacity of the river.

Step 7: HEC-RAS output include contraction scour, pier scour, abutment scour and combined scour.

RESULTS AND DISCUSSION

Using the methodology discussed, the scour around existing piers of Sardar Bridge was computed for various discharges and for eight different dual bridge cases. The dual bridge analysis is carried out for four bridges on the upstream side and four downstream located exactly side to side with each other along the existing bridge. The existing bridge has a deck width of 22.4 meters. So, the distance of the bridges placed side by side to each other from the existing bridge will be 11.2 m, 56 m, 110.8 m and 145.6 m upstream and downstream. The analysis is repeated using dual bridges upstream and downstream of the existing bridge at 11.2 m, 56 m, 100.8 m, and 145.6 m distances.

Existing bridge (Sardar Bridge)

Figure 6 shows the position of the existing Sardar Bridge and cross-section along the river length. The flow discharges 8501, 25788, 33257 and 43924 cumecs were used to determine scour depth around bridge piers. The computed contraction scour and pier scour in HEC-RAS is listed in Table 2. From the table it has been observed that velocity and scour depth increase with increase in discharge whereas the pier scour depth increases for 8501, 25788 and 33257 cumecs and decreases for 43924 cumecs. The reduction in velocity and scour depth observed may be due to the overtopping of water on the bridge deck at large discharge. Table 3 shows the values of abutment scour and combined scour. Results reflects an increment in the abutment scour at the existing bridge with increasing discharge.

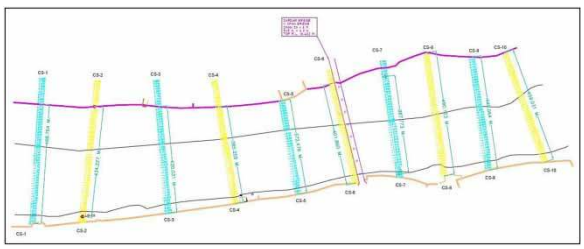

Figure 6 | Existing bridge.

Table 2 | Contraction and pier scour at Sardar Bridge (existing bridge)

	Contraction Scour				Pier Scour (All Piers)	
Flow Profile (m^3/s)	Parameters	Left	Channel	Right	Ys (m)	Fr
PF 1	Ys (m)	2.21	3.52	4.37	12.6	0.5
25788	Vc (m/s)	1.32	1.41	1.31		
PF 2	Ys (m)	–	–	–	13.18	0.49
33257	Vc (m/s)	–	–	–		
PF 3	Ys (m)	6.53	9.65	9.94	12.95	0.36
43924	Vc (m/s)	1.47	1.52	1.46		
PF 4	Ys (m)	0.8	2.14	2.12	9.93	0.42
8501	Vc (m/s)	1.15	1.3	1.15		

PF: Flow profile; Ys: Scour depth; Fr: Froude number; Vc: Critical velocity.

Table 4 shows the relationship between scour depth and the Froude number on the existing bridge. There is a rise in Froude number for 8501 and 25788 cumecs. For the discharge of 33257 cumecs the water level reaches to the deck of the bridge and due to this scour depth increases whereas Froude's number decreases. The scour depth and the Froude's number decrease further for the 43924 cumecs of discharge as the water level overtopped to the deck of the bridge. Figures 7(a), 7(b), 8(a) and 8(b) each present a graphical representation of local scour, contraction scour, pier scour, abutment scour and combined scour.

Effect of upstream adjacent bridge on Sardar Bridge

In this section, analysis of the existing bridge is carried out when a new adjacent bridge upstream is proposed. The following four cases have been analysed in detail: Case-I: Proposed bridge located at 11.2 m distance from Sardar Bridge, Case-II: Proposed bridge located at 56 m distance from Sardar Bridge, Case-III: Proposed bridge located at 100.8 m distance

Table 3 | Abutment and combined scour at Sardar Bridge (existing bridge)

	Abutment Scour			Combined Scour Depths			
Flow Profile (m^3/s)	**Parameters**	**Left**	**Right**	**Left (m)**	**Channel (m)**	**Left abut + Contr (m)**	**Right abut + Contr (m)**
PF 1	Ys (m)	39	12.79	14.82	16.12	41.22	17.16
25788	Vc (m/s)	0.52	1.02				
PF 2	Ys (m)	51.37	40.93	–	–	–	–
33257	Vc (m/s)	0.5	0.38				
PF 3	Ys (m)	79.24	49.11	19.48	22.60	85.77	59.05
43924	Vc (m/s)	0.3	0.27				
PF 4	Ys (m)	7.64	–	10.73	12.07	8.44	–
8501	Vc (m/s)	0.59	–				

PF: Flow profile; Ys: Scour depth; Vc: Critical velocity.

Table 4 | Scour depth and Froude's number on existing bridge

Serial No.	Scour Depth (m)	Froude's Number	Flow (m^3/s)
1	9.93	0.42	8501
2	12.6	0.5	25788
3	13.18	0.49	33257
4	12.95	0.36	43924

from Sardar Bridge, Case-IV: Proposed bridge located at 145.6 m distance from Sardar Bridge. Effect of adjacent bridge is analyzed to evaluate the scour depth on the existing bridge for discharge of 33257 cumecs (1944), 25788 cumecs (2006), 43924 cumecs (1968) flood events and 8501 cumecs which is the carrying capacity of the river.

Case-I: proposed bridge located at 11.2 m distance from Sardar Bridge (existing bridge)

From the analysis it has been observed that due to the presence of an adjacent bridge on the upstream side of the existing bridge, there is a decrease in the Froude's number and subsequent decrease in the scour depth for carrying

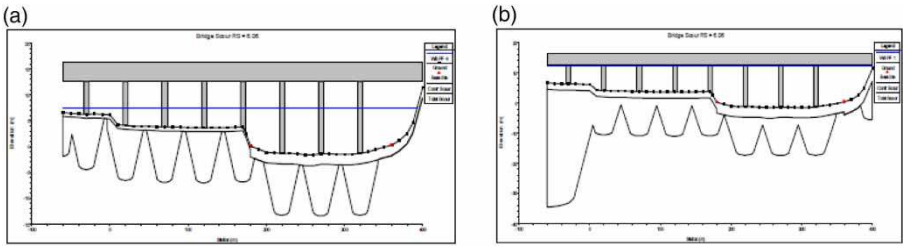

Figure 7 | (a) Scour depth for 8501 cumecs discharge, (b) Scour depth for 25788 cumecs discharge.

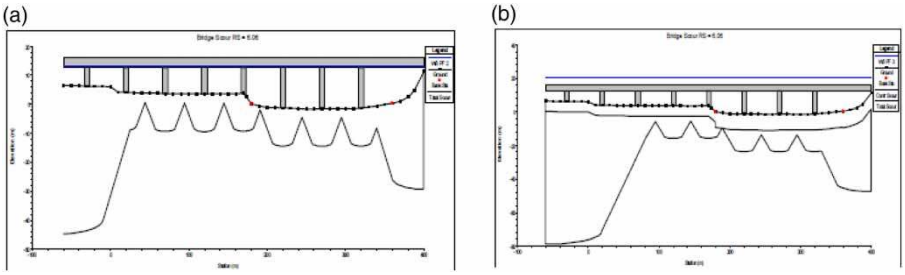

Figure 8 | (a) Scour depth for 33257 cumecs discharge, (b) Scour depth for 43924 cumecs discharge.

capacity and the flood events compared to with the existing bridge only. Table 5 shows scour depth, Froude's number and variation in both, compared with the existing single bridge scenario. When the adjacent bridge is placed on the upstream side at 11.2 m from the existing bridge, most of the frictional resistance offered by water is exerted on the upstream bridge pier. Due to this, frictional resistance on the existing bridge pier is lower, hence a negative variation is observed in both Froude number and scour depth.

Case-II: proposed bridge located at 56 m distance from Sardar Bridge (existing bridge)

From the analysis, it has been observed that due to the presence of an adjacent bridge on the upstream side of the existing bridge, there is a decrease in Froude's number and subsequent decrease in the scour depth for carrying capacity and flood events compared to with the existing bridge only. Table 6 shows scour depth, Froude's number and variation in both, compared with the existing single bridge situation. When the adjacent bridge is placed upstream at 56 m from the existing bridge, most of the frictional resistance offered by water is exerted on the upstream bridge pier. Due to this, frictional resistance on the existing bridge pier is less, hence negative variation is observed in both the Froude number and scour depth.

Table 5 | Scour depth and Froude's number at existing bridge when adjacent upstream bridge at a distance of 11.2 m

Sr. No.	Flow (m^3/s)	Scour depth (m)	Froude's number	Variation in scour depth	Variation in Froude's number
1	8501	9.74	0.39	−ve	−ve
2	25788	12.44	0.47	−ve	−ve
3	33257	12.85	0.44	−ve	−ve
4	43924	12.79	0.34	−ve	−ve

Table 6 | Scour depth and Froude's number at existing bridge when adjacent upstream bridge at a distance of 56 m

Sr. No.	Flow (m^3/s)	Scour depth (m)	Froude's number	Variation in scour depth	Variation in Froude's Number
1	8501	9.74	0.39	−ve	−ve
2	25788	12.45	0.48	−ve	−ve
3	33257	12.84	0.44	−ve	−ve
4	43924	12.79	0.34	−ve	−ve

Case-III: proposed bridge located at 100.8 m distance from Sardar Bridge (existing bridge)

From the analysis, it has been observed that due to the presence of an adjacent bridge on the upstream side of the existing bridge, there is a decrease in Froude's number and subsequent decrease in the scour depth for carrying capacity and the flood events compared to with the existing bridge only. Table 7 shows scour depth, Froude's number and variation in both, compared with the existing single bridge condition. When the adjacent bridge is placed upstream at 100.8 m from the existing bridge, most of the frictional resistance offered by water is exerted on the upstream bridge pier. Due to this, frictional resistance on existing bridge pier is reduced, hence a negative variation is observed in both Froude number and scour depth.

Case-IV: proposed bridge located at 145.6 m distance from Sardar Bridge (existing bridge)

From the analysis, it has been observed that due to the presence of an adjacent bridge on the upstream side of the existing bridge, there is a decrease in Froude's number and subsequent decrease in the scour depth for carrying capacity and the flood events, compared to with the existing bridge only. Table 8 shows scour depth, Froude's number and variation in both, compared with the existing single bridge scenario. When the adjacent bridge is placed upstream at 145.6 m from the existing bridge, most of the frictional resistance offered by water is exerted on the upstream bridge pier.

Table 7 | Scour depth and Froude's number at existing bridge when adjacent upstream bridge at a distance of 100.8 m

Sr. No.	Flow (m^3/s)	Scour depth (m)	Froude's number	Variation in scour depth	Variation in Froude's Number
1	8501	9.74	0.39	−ve	−ve
2	25788	12.45	0.48	−ve	−ve
3	33257	12.84	0.44	−ve	−ve
4	43924	12.79	0.34	−ve	−ve

Table 8 | Scour depth and Froude's number at existing bridge when adjacent upstream bridge at a distance of 145.6 m

Sr. No.	Flow (m^3/s)	Scour depth (m)	Froude's number	Variation in scour depth	Variation in Froude's Number
1	8501	9.74	0.39	−ve	−ve
2	25788	12.45	0.48	−ve	−ve
3	33257	12.84	0.44	−ve	−ve
4	43924	12.79	0.34	−ve	−ve

Due to this, frictional resistance on the existing bridge pier is reduced, hence negative variation is observed in both the Froude number and scour depth.

From Figures 9(a) and 9(b), it is evident that for all the cases on the upstream side of the existing bridge, the Froude number as well as scour depth decreases with increasing discharge. Particularly for Case-I (11.2 m distance from existing bridge) the value of Froude's number and scour depth for discharge of 25788 cumecs is found to be minimum for all cases compared with the existing single bridge scenario. For 33257 cumecs of discharge, scour depth is found to be maximum compared to all other cases on the upstream side of the existing bridge.

Effect of downstream adjacent bridge on Sardar Bridge

In this section, analysis of the existing bridge is carried out when new bridge adjacent and downstream is proposed. The following four cases have been analysed in detail: Case-I: Proposed bridge located at 11.2 m distance from Sardar Bridge, Case-II: Proposed bridge located at 56 m distance from Sardar Bridge, Case-III: Proposed bridge located at 100.8 m distance from Sardar Bridge, Case-IV: Proposed bridge located at 145.6 m distance from Sardar Bridge. The effect of an adjacent bridge was analyzed to evaluate the scour depth on the existing bridge for discharge of 33257 cumecs (1944), 25788 cumecs (2006), 43924 cumecs (1968) flood events and for 8501 cumecs which is the carrying capacity of the river.

Case-I: proposed bridge located at 11.2 m distance from Sardar Bridge (existing bridge)

From the analysis it is observed that due to the presence of an adjacent bridge on the downstream side of the existing bridge, there is an increase in Froude's number and scour depth for the 8501 and 25788 cumecs flood events whereas for the 33257 and 43924 cumecs flood events Froude's number and scour depth decreases as compared to the results for the Sardar Bridge only. Table 9 shows scour depth, Froude's number and variation in both, compared with the existing single bridge scenario. When the adjacent bridge is placed downstream at 11.2 m from the existing bridge, most of the frictional resistance offered by water was exerted on the existing bridge pier. Due to this, frictional resistance is more which results in a positive variation in Froude number and scour depth for 8501 and 25788 cumecs but negative variation for higher discharges.

Case-II: proposed bridge located at 56 m distance from Sardar Bridge (existing bridge)

From the analysis it is observed that due to the presence of an adjacent bridge on the downstream side of the existing bridge, there is an increase in Froude's number and scour depth for the 8501 and 25788 cumecs flood events whereas for the 33257 and 43924 cumecs flood events Froude's

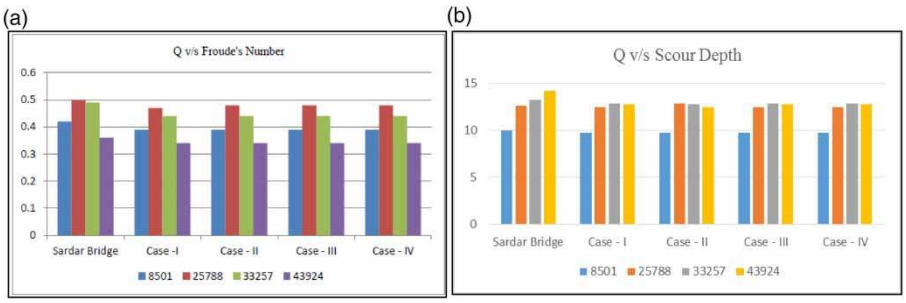

Figure 9 | (a) Discharge v/s Froude's number for all cases upstream, (b) Discharge v/s Scour Depth for all cases upstream.

Table 9 | Scour depth and Froude's number at existing bridge when adjacent downstream bridge at a distance of 11.2 m

Sr. No.	Flow (m^3/s)	Scour depth (m)	Froude's number	Variation in scour depth	Variation in Froude's Number
1	8501	10.36	0.48	+ve	+ve
2	25788	12.93	0.54	+ve	+ve
3	33257	12.99	0.36	−ve	−ve
4	43924	12.85	0.34	−ve	−ve

number and scour depth decreases as compared to the results for the Sardar Bridge only. Table 10 shows scour depth, Froude's number and variation in both, compared with the existing single bridge scenario. When the adjacent bridge is placed downstream at 56 m from the existing bridge, most of the frictional resistance offered by water was exerted on the existing bridge pier.

Case-III: proposed bridge located at 100.8 m distance from Sardar Bridge (existing bridge)

From the analysis it is observed that due to the presence of an adjacent bridge on the downstream side of the existing bridge, there is an increase in Froude's number and scour depth for the 8501, 25788 and 33257 cumecs flood events, whereas for the 43924 cumecs flood event Froude's number is the same and scour depth increases as compared to results for the Sardar Bridge only. Table 11 shows scour depth, Froude's number and variation in both, compared with the existing single bridge scenario. When the adjacent bridge is placed downstream at 100.8 m from the existing bridge, most of the frictional resistance offered by water was exerted on the existing bridge pier.

Table 11 | Scour depth and Froude's number at existing bridge with adjacent downstream bridge at a distance of 100.8 m

Sr. No.	Flow (m^3/s)	Scour depth (m)	Froude's number	Variation in scour depth	Variation in Froude's Number
1	8501	11.49	0.48	+ve	+ve
2	25788	12.91	0.54	+ve	+ve
3	33257	13.45	0.52	+ve	+ve
4	43924	12.99	0.36	+ve	same

Case-IV: proposed bridge located at 145.6 m distance from Sardar Bridge (existing bridge)

From the analysis it is observed that due to the presence of an adjacent bridge on the downstream side of the existing bridge, there is an increase in Froude's number and scour depth for the 8501, 25788 and 33257 cumecs flood events, whereas for the 43924 cumecs flood event Froude's number decreases and scour depth increases as compared to the results for the Sardar Bridge only. Table 12 shows scour depth, Froude's number and variation in both, compared with the existing single bridge scenario. When the adjacent bridge is placed downstream at 145.6 m from the existing bridge, most of the frictional resistance offered by water was exerted on the existing bridge pier.

From Figures 10(a) and 10(b), it can be observed that for Case-I (11.2 m distance from existing bridge) the value of Froude's number and scour depth for 8501 and 25788 is increasing and further increase in discharge shows a lesser value of Froude's number and scour depth. For the remaining cases, the value of Froude's number remains stable at 0.48, 0.54, 0.52 and 0.36 for 8501, 25788, 33257 and 43924 cumecs of discharge respectively. Scour depth is

Table 10 | Scour depth and Froude's number at Existing Bridge when adjacent downstream bridge at a distance of 56 m

Sr. No.	Flow (m^3/s)	Scour depth (m)	Froude's number	Variation in scour depth	Variation in Froude's Number
1	8501	10.35	0.48	+ve	+ve
2	25788	12.92	0.54	+ve	+ve
3	33257	13.47	0.53	+ve	+ve
4	43924	12.99	0.36	+ve	same

Table 12 | Scour depth and Froude's number at existing bridge with adjacent downstream bridge at a distance of 145.6 m

Sr. No.	Flow (m^3/s)	Scour depth (m)	Froude's number	Variation in scour depth	Variation in Froude's Number
1	8501	10.34	0.48	+ve	+ve
2	25788	12.90	0.53	+ve	+ve
3	33257	13.44	0.52	+ve	+ve
4	43924	14.42	0.35	+ve	−ve

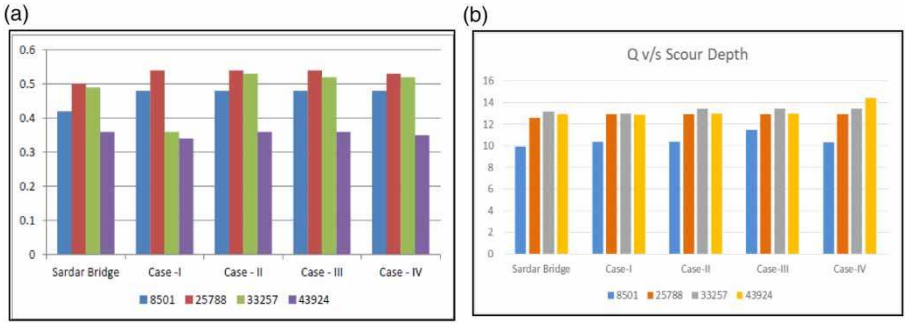

Figure 10 | (a) Discharge v/s Froude's number for all cases (downstream), (b) Discharge v/s Scour depth for all cases (downstream).

found to increase with increase in distance of the proposed bridge from the existing bridge for all discharge.

SUMMARY AND CONCLUSION

Results indicate that scour prediction is significantly affected by spatial distribution of flow field, especially the angle of alignment with bridge piers. For a bridge with multiple piers, the spatial effects of flow field distribution are also considered, but a 1D model such as HEC-RAS is incapable of realistically simulating such distribution of flow field. In the present study after analysis, it has been observed that as the discharge increases from 8501 cumecs to 25788 cumecs the scour depth decreases if the adjacent bridge is on the upstream side whereas downstream of the existing bridge there is an increase in Froude's number and scour depth. When discharge increased from 25788 cumecs to 33257 cumecs it was revealed that Froude's number and scour depth decreased subsequently upstream, whereas downstream up to 11.2 m from the existing bridge Froude number and the scour depth decrease; after 11.2 m from the existing bridge Froude's number and scour depth both increase. Also, when discharge increased from 33257 cumecs to 43924 cumecs it was observed that Froude's number and scour depth decrease upstream, whereas downstream up to 11.2 m from the existing bridge section Froude number and the scour depth decreases but more than 11.2 m from the existing bridge Froude's number and scour depth both increase. Increasing discharge significantly affects the Froude's number and scour depth upstream and downstream of the bridges.

Scour depth analysis in case of parallel bridges was carried out using HEC-RAS. The difference between the computed local scour depth on the existing and adjacent bridge showed that the HEC-RAS model is a prominent tool for simulating local scour depth in case of dual bridges. On the upstream side, the proposed adjacent bridge should be located at a distance of 100.8 m or more from the existing bridge which would have a minimum effect on Froude's number and scour depth. Whereas on the downstream side, the Froude's number and scour depth decrease for a proposed adjacent bridge located at 11.2 m from the existing bridge. Further increasing the distance more than 11.2 m on the downstream side for the proposed adjacent bridge from the existing bridge, Froude number increases with increase in the scour depth. By comparing both cases i.e. upstream as well downstream, it is more advisable to construct the proposed adjacent bridge upstream instead of on the downstream side of the existing bridge. The existing bridge is old and its hydraulic stability should be assured when another bridge parallel to the existing bridge is proposed to be constructed. It is advisable to place it on the upstream side at any distance from the existing bridge as the Froude number and scour depth decrease on the existing bridge pier for all the flow conditions. HEC-RAS software predicts the scour depth but not the rate and time of scour.

DATA AVAILABILITY STATEMENT

All relevant data are included in the paper or its Supplementary Information.

REFERENCES

Afzali, S. H. 2016 New model for determining local scour depth around piers. *Arabian Journal for Science and Engineering* **41** (10), 3807–3815.

Ansari, S. A. & Qadar, A. 1994 Ultimate depth of scour around bridge piers. In *Hydraulic Engineering*. ASCE, pp. 51–55.

Azamathulla, H. M., Ab Ghani, A., Zakaria, N. A. & Guven, A. 2013 Erratum for 'Genetic programming to predict bridge pier scour' by H. Md. Azamathulla, Aminuddin Ab Ghani, Nor Azazi Zakaria, and Aytac Guven. *Journal of Hydraulic Engineering* **139** (9), 1020–1020.

Baker, C. J. 1980 Theoretical approach to prediction of local scour around bridge piers. *Journal of Hydraulic Research* **18** (1), 1–12.

Beg, M. & Beg, S. 2013 Scour reduction around bridge piers: a review. *International Journal of Engineering Inventions* **2** (7), 7–15.

Brandimarte, L., Paron, P. & Di Baldassarre, G. 2012 Bridge pier scour: a review of processes. *Measurements and Estimates. Environmental Engineering & Management Journal (EEMJ)* **11** (5), 975–989.

CDOT 2019 Chapter 17 (Bank protection). In: *Drainage Design Manual*. Colorado Department of Transportation, Denver, Colorado, USA. See: https://www.codot.gov/business/hydraulics/drainage-design-manual/chapter17_bankprotection.pdf.

Cunha, L. V. 1975 Time evolution of local scour. In *Proceedings 16th International Association for Hydraulic Research Congress*, Vol. 2, 27 July to 1 Aug, Sao Paulo, Brazil, pp. 285–299.

Dahe, P. D. & Kharode, S. B. 2015 Evaluation of scour depth around bridge piers with various geometrical shapes. *Evaluation* **2** (7), 41–48.

Debnath, K., Chaudhuri, S. & Manik, M. K. 2014 Local scour around abutment in clay/sand-mixed cohesive sediment bed. *ISH Journal of Hydraulic Engineering* **20** (1), 46–64.

Devi, Y. S. & Barbhuiya, A. K. 2017 Bridge pier scour in cohesive soil: a review. *Sādhanā* **42** (10), 1803–1819.

Feng, C. W., Ju, S. H., Huang, H. Y. & Chang, P. S. 2011 Using genetic algorithms to estimate the scour depth around the bridge pier. In *Proc. 28th International Symposium on Automation and Robotics in Construction*, pp. 514–519.

Gaudio, R., Grimaldi, C., Tafarojnoruz, A. & Calomino, F. 2010 Comparison of formulae for the prediction of scour depth at piers. In *Proc., 1st IAHR European Division Congress*. Heriot-Watt University, Edinburgh, UK.

Ghanbari, A. E. & Kashefipour, D. M. 2017 *Estimation of Scour Depth at Bridge Piers by Using FASTER Model and Experimental Formulas*.

Goel, A. 2015 Predicting bridge pier scour depth with SVM. *World Academy of Science, Engineering and Technology, International Journal of Civil, Environmental, Structural, Construction and Architectural Engineering* **9** (2), 211–216.

Govindasamy, A. V., Briaud, J. L., Kim, D., Olivera, F., Gardoni, P. & Delphia, J. 2010 Observational method for estimating future scour depth at existing bridges. In: *Scour and Erosion: Proceedings 5th International Conference on Scour and Erosion (ICSE-5)*. November 7–10, 2010, San Francisco, pp. 41–65.

Hamidifar, H. & Omid, M. H. 2017 Local scour of cohesive beds downstream of a rigid apron. *Canadian Journal of Civil Engineering* **44** (11), 935–944.

Johnson, P. A., Clopper, P. E., Zevenbergen, L. W. & Lagasse, P. F. 2015 Quantifying uncertainty and reliability in bridge scour estimations. *Journal of Hydraulic Engineering* **141** (7), 04015013.

Kandasamy, J. K. & Melville, B. W. 1998 Maximum local scour depth at bridge piers and abutments. *Journal of Hydraulic Research* **36** (2), 183–198.

Kester, J. G. & Davis, S. R. 2010 Hydraulic Variables for Scour Using HEC-RAS. In *Scour and Erosion*, pp. 1120–1129.

Kumar, A. & Kothyari, U. C. 2004 Effect of stream-wise spacing of bridge piers on scour depth. In *Proceedings 2nd International Conference on Scour and Erosion (ICSE-2)*, November 14.–17., 2004, Singapore.

Link, O., García, M., Pizarro, A., Alcayaga, H. & Palma, S. 2020 Local scour and sediment deposition at bridge piers during floods. *Journal of Hydraulic Engineering* **146** (3), 04020003.

Liu, H., Zhou, J. G. & Burrows, R. 2009 Numerical modeling of turbulent compound channel flow using the lattice Boltzmann method. *International Journal for Numerical Methods in Fluids* **59** (7), 753–765.

MacBroom, J. G. 2012 Bridge scour and sediment analysis for river restoration projects. In: *World Environmental and Water Resources Congress 2012: Crossing Boundaries*, May 20–24, 2012, New Mexico, United States, pp. 2521–2531.

Mousavi, F. & Daneshfaraz, R. 2013 Evaluating Various Factors in Calculation of Scour Depth around Bridge Piers using HEC-RAS Software, CSU2001 and Froehlich Equations.

Neerukatti, R. K., Kim, I., Fard, M. Y. & Chattopadhyay, A. 2013 Prediction of scour depth around bridge piers using Gaussian process, Vol. 8692. In *Proc. of SPIE Vol*, pp. 86922Z-1.

Nou, M. R. G., Moghaddam, M. A., Bajestan, M. S. & Azamathulla, H. M. 2020 Control of bed scour downstream of ski-jump spillway by combination of six-legged concrete elements and riprap. *Ain Shams Engineering Journal* **1** (1), 1–13.

Pandey, M., Sharma, P. K., Ahmad, Z. & Karna, N. 2018a Maximum scour depth around bridge pier in gravel bed streams. *Natural Hazards* **91** (2), 819–836.

Pandey, M., Sharma, P. K., Ahmad, Z. & Singh, U. K. 2018b Experimental investigation of clear-water temporal scour variation around bridge pier in gravel. *Environmental Fluid Mechanics* **18** (4), 871–890.

Pandey, M., Azamathulla, H. M., Chaudhuri, S., Pu, J. H. & Pourshahbaz, H. 2020a Reduction of time-dependent scour around piers using collars. *Ocean Engineering* **213**, 107692.

Pandey, M., Oliveto, G., Pu, J. H., Sharma, P. K. & Ojha, C. S. 2020b Pier scour prediction in non-uniform gravel beds. *Water* **12** (6), 1696.

Rodriguez, A., Brea, D., Farías, D., Bravo, H. R., Castelló, E., Hillman, G. & Spalletti, P. 2003 Hydraulic analyses for a new bridge over the Parana River, Argentina. *International Journal of Sediment Research* **18** (2), 166–175.

Singh, R. K., Pandey, M., Pu, J. H., Pasupuleti, S. & Villuri, V. G. K. 2020 Experimental study of clear-water contraction scour. *Water Supply* **20** (3), 943–952.

Tyagi, A. K. 2001 Scour Modeling of Black Bear Creek Bridge on Cimarron Turnpike, Oklahoma. In *Bridging the Gap: Meeting the World's Water and Environmental Resources Challenges*, pp. 1–9.

Yanmaz, A. M. & Bulut, F. 2001 Computer aided analysis of flow through river bridges. In *Bridging the Gap: Meeting the World's Water and Environmental Resources Challenges*, pp. 1–9.

Yanmaz, A. M. & Kose, O. 2007 Surface characteristics of scouring at bridge elements. *Turkish Journal of Engineering and Environmental Sciences* **31** (2), 127–134.

Yu, X. & Yu, X. B. 2008 1D and 2D Hydraulic Simulations for Bridge Scour Prediction: A Comparative Study. In *The Fourth International Conference on Scour and Erosion*, Nov, pp. 5–7.

Yu, X., Tao, J. & Yu, X. 2011 Comparison Study on Computer Simulations for Bridge Scour Estimation. In: *Geo-Risk 2011: Risk Assessment and Management*, June 26–28, 2011, Atlanta, GA, United States, pp. 1125–1132.

Yusoff, M. A. M., Azamathulla, H. M. & Ghani, A. A. 2016 Time variations of scour below submerged skewed pipelines. *MS&E* **136** (1), 012071.

First received 28 July 2020; accepted in revised form 27 September 2020. Available online 15 October 2020